RSC Advances

This is an *Accepted Manuscript*, which has been through the Royal Society of Chemistry peer review process and has been accepted for publication.

Accepted Manuscripts are published online shortly after acceptance, before technical editing, formatting and proof reading. Using this free service, authors can make their results available to the community, in citable form, before we publish the edited article. This *Accepted Manuscript* will be replaced by the edited, formatted and paginated article as soon as this is available.

You can find more information about *Accepted Manuscripts* in the Information for Authors.

Please note that technical editing may introduce minor changes to the text and/or graphics, which may alter content. The journal's standard Terms & Conditions and the Ethical guidelines still apply. In no event shall the Royal Society of Chemistry be held responsible for any errors or omissions in this *Accepted Manuscript* or any consequences arising from the use of any information it contains.

ROYAL SOCIETY OF CHEMISTRY

www.rsc.org/advances

Journal Name

RSCPublishing

ARTICLE

A double-layer moisture barrier & antireflective film based on bridged polysilsesquioxane and porous silica

Cite this: DOI: 10.1039/xoxxoooooox

Cong Zhang,[a,b] Ce Zhang,[a,b] Jinghua Sun,[a,b] Ruimin Ding,[a] Qinghua Zhang[c] and Yao Xu*[,a]

Received ooth January 2012,
Accepted ooth January 2012

DOI: 10.1039/xoxxoooooox

www.rsc.org/

A double-layer film with both moisture barrier protective and antireflective (AR) abilities was prepared. The upper layer was a porous silica AR film. The bottom layer was a nonporous bridged polysilsesquioxane (BPSQ) moisture barrier protective film based on the sol-gel process of a newly synthesized X-bridged silsesquioxane (EG-BPSQ) monomer. The EG-BPSQ monomer was synthesized via the stoichiometric reaction between 3-glycidoxypropyltrimethoxysilane (GPTMS) and ethylene diamine (EDA) at 60 °C with no catalyst. The high polycondensation of inorganic matrix and the special X-bridging organic chain in EG-BPSQ resulted in the dense structure of the protective film. Transmittance of KH_2PO_4 (KDP) crystal coated with EG-BPSQ film only declined 1.11% at 1053 nm wavelength and 1.49% at 351 nm wavelength after tested in 60% humidity environment for 100 days, indicating that the EG-BPSQ protective film possessed excellent moisture barrier performance for KDP crystal. For the double-layer film coated on KDP crystal, good AR performance was obtained: 98.09% at 1053 nm wavelength and 99.51% at 351 nm wavelength.

Introduction

Moisture permeation is a serious problem in gas separation and storage, packaging, and protective coatings.[1-3] Therefore, there were many reports on controlling moisture permeation through moisture barrier protection. KDP crystal is a common optical crystal used as frequency converter in laser system.[4-6] As an easy deliquescent material, it needs moisture barrier protection to avoid the decrease of its optical transmittance in humidity environment. Various approaches have been reported to prepare moisture barrier protective film for KDP crystal, which can be classified into two kinds. The traditional strategy was based on the hydrophobic functional groups in film to prevent moisture permeation.[7-10] This kind of hydrophobic film could be achieved by treating the film with hydrophobic agents or adopting hydrophobic medium into the film. The most effective hydrophobic medium was fluorine. Floch and Belleville developed a moisture barrier and antireflective film with good moisture barrier property by coating a layer of Teflon AF2400 (DuPont product) on the surface of a porous silica film.[11] Unfortunately, although the introduction of the Teflon AF2400 could greatly improve the moisture barrier property of films, and had no influence on the film optical property, the preparation process cost so much and was easy to cause the organic fluorine pollution.

Another moisture barrier film preparation used dense and nonporous materials to stop or delay the permeation of moisture. BPSQ is a popular organic-inorganic hybrid material used to prepare dense material.[12-15] It can be obtained by the hydrolysis and condensation of the corresponding bridged silsesquioxane monomers. There are three methods to prepare the monomer. However, the metalation and hydrosilylation reaction need introduce catalysts, which might lead to the laser-induced damage threshold of the film, for they are difficult to be removed from the reaction system. Therefore, the functionalization of organo-trialkoxysilane seems to be the ideal choice, for it can carry on without catalyst. Hu et.al reported a serial transparent moisture barrier protective film for $NiSO_4 \cdot 6H_2O$ crystal (a general UV filter) based on several diisocyanate-bridged polysilsesquioxanes.[16] But the lots of uramido groups in film were very easy to be decomposed by UV light, which resulted in instability under UV lasers. Therefore, we design a new BPSQ without unsaturated groups to prepare moisture barrier protective film.

GPTMS was selected as the inorganic structure silica source because it has no unsaturated group and the epoxy group in GPTMS could be opened by amine to form organic-inorganic hybrid materials, which have properties (e.g., compact structure，excellent adhesion strength, high hardness, good flexibility, and stable in organic solvent) similar to the

RSC Advances Accepted Manuscript

epoxy resin cured product.[17-19] Several of these properties are exactly what a moisture barrier protective film required. However, GPTMS was rarely reported to be employed to prepare moisture barrier protective film for optical crystal. Therefore, in this work, we choose GPTMS and EDA to synthesize a new BPSQ monomer with an X-shape cross-linking among four trimethoxylsilyl groups. With this monomer, a special BPSQ was obtained through its hydrolysis and condensation and was denoted as EG-BPSQ. Subsequently, protective film was deposited on KDP crystal using EG-BPSQ sol.

The introduction of EDA was benefit to form a higher degree of crosslinking network structure, for one EDA molecular could join four GPTMS molecular together, and the organic bridging chain became more complex. Consequently, it was easier to form the dense structure after the bending and winding of organic chain in the inorganic silica framework. Besides, there was no catalyst was introduced in the synthesize process of EG-BPSQ monomer, and there was no unsaturated groups present in the molecular structure of EG-BPSQ. Even better, the EG-BPSQ protective film matched well with substrates and porous silica AR film. Therefore, the double-layer system which adopting the EG-BPSQ film as the bottom layer and the porous silica AR film as the upper layer could simultaneously satisfy the requirement in moisture barrier, antireflection and the laser-induced damage resistance of KDP crystal.

Experiment section

Materials: 3-Glycidoxypropyltrimethoxysilane (GPTMS, 99%) and tetraethyl orthosilicate (TEOS, 99%) were purchased from Acros Company. Ethylene diamine (EDA, 99%), anhydrous ethanol (EtOH) and ammonia water (27%, wt.%) were purchased from Sinopharm Chemical Reagent Co., Ltd. KDP crystal (50 × 50 × 8 mm^3) were purchased from Fujian Institute of Research on the Structure of Matter, Chinese Academy of Sciences. All these were used as received. Water was deionized and twice distilled.

Synthesis of the EG-BPSQ monomer: The synthesis was in a three necked flask of 300 ml, employing a molar ratio of GPTMS/EDA = 4. The flask was sealed under nitrogen, placed in a thermostat at 60℃ and then stirred for 72 hours. The completion of reaction was characterized by Fourier-transformed Infrared (FT-IR) spectra. EtOH was used as solvent, and the concentration of the monomer was 0.1 mol·L^{-1}. For a clear description, the synthesis process was illustrated by Scheme 1.

Synthesis of the EG-BPSQ sol: Using EG-BPSQ monomer, a special sol was synthesized through the hydrolysis and condensation of EG-BPSQ and was denoted as EG-BPSQ sol. The detailed synthesis was performed in a flask using an aqueous solution of ammonia as catalyst. The reactants were mixed with a molar ratio of H_2O : NH_3 : Si = 3 : 1.07 : 1 in anhydrous EtOH. The flask was sealed and placed in a thermostat, stirred at 60℃ and aged for 48 hours. The final product was a colorless and transparent solution, in which the EG-BPSQ monomer molecules cross-linked into 3D networks, as shown in scheme 1.

Scheme 1. Synthesis of bridged monomer and EG-BPSQ.

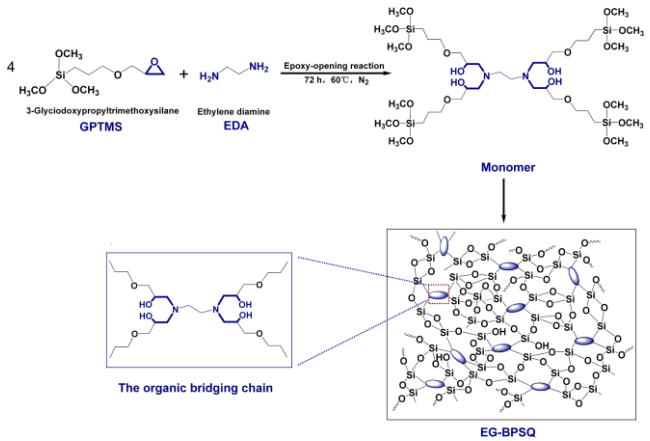

Preparation of the silica sol: The silica sol used for AR film was prepared by ammonia catalyzed hydrolysis and condensation of TEOS in anhydrous ethanol. The reactants were mixed with a molar ratio of TEOS : H_2O : NH_3 : EtOH = 1 : 2.8 : 0.3 : 23. The sol was left to react under stirring at room temperature for 2 hours. After aging for 48 hours at room temperature, the final silica sol became a transparent light blue suspension.

Preparation of films: KDP crystal substrates were cleaned with toluene before use. KDP crystal was immersed in EG-BPSQ sol for 1 min in clear air at 25℃ and RH 30%-40%, and withdrawn from the sol at a speed of 150 mm·min^{-1}. The as-prepared film was dried for 24 hours at room temperature and noted as EG-BPSQ film. Its thickness was around 100 nm. Then, KDP crystal coated with EG-BPSQ film was immersed in the silica sol for 1 min, and withdrawn from the sol at different speed to obtain films with central wavelength at 1053 nm and 351 nm respectively. Finally, the as-prepared film was dried for 10 min at room temperature and noted as the moisture barrier & AR film. The packing structure of the double-layer film was showed in Scheme 2.

Scheme 2. Structure of the double-layer protective & antireflective film.

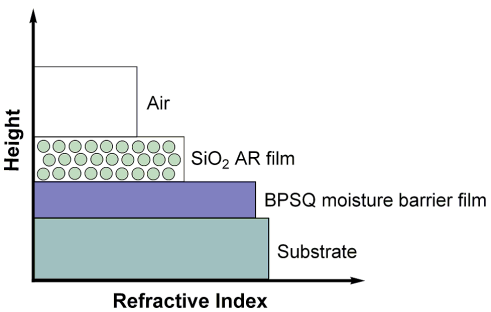

Characterization: The chemical structure of the EG-BPSQ monomer and BPSQ were characterized by FT-IR and Nuclear Magnetic Resonance (NMR). FT-IR spectra were recorded on a Nicolet IS50 spectrometer using a DTGS detector with the transmittance mode. ^{13}C NMR spectra were recorded on a

RSC Advances Accepted Manuscript

This journal is © The Royal Society of Chemistry 2012

Bruker AVANCE IIITM 400MHz (solution) spectrometer. EDA, GPTMS and EG-BPSQ monomer were dissolved in $CDCl_3$. To characterize the synthesized EG-BPSQ, it was dried to obtain the gel. The BPSQ gel was then subjected to ^{29}Si MAS NMR on Bruker AVANCE IIITM 600 MHz spectrometer using a 7 mm probe under magic-angle spinning.

To measure the porosity of protective film, EG-BPSQ sol was dip-coated on the glass substance repeatedly until the films were thick enough to be scratched off for the N_2 adsorption-desorption measurement on a Micromeritics TriStar 3000 physisorption analyzer.

The anti-ultraviolet radiation performance of the film was tested by a 300 W Xenon lamp (PLS-SXE300, Perfectlight) with wavelength range of 250 nm to 380 nm for 3 h, 6 h, 9 h an d 12 h. A filter was used to cut off the visible light from the Xenon lamp.

The surface morphology and roughness of films were measured on an atomic force microscope (AFM, PSIA XE-100). The root mean square roughness (Rq) of the film was calculated with XEI software. The cross-section morphology of the film were observed on a scanning electron microscopy (SEM, JEOL JSM-7001F, gold-coated samples). The water contact angle of films was measured on a contact-angle meter (SL200B).

The optical transmittance of the film was recorded on a UV-Visible-NIR spectrometer (UV-4100, Hitachi) with the transmittance mode, in the wavelength range of 240 - 1200 nm. The refractive index and physical thickness of film were measured on a spectroscopic ellipsometer (SC620, Sanco) at 60° incidence, and the results were fitted with Cauchy model.

The abrasion-resistance property of the protective film was tested using an abrasion-resistance machine (Linear Abraser 5700, Taber Industries). The films were rubbed for 30 cycles by CF-10 abraser with rate of 5 cycles per minute.

Results and discussion

Chemical structure of the EG-BPSQ monomer

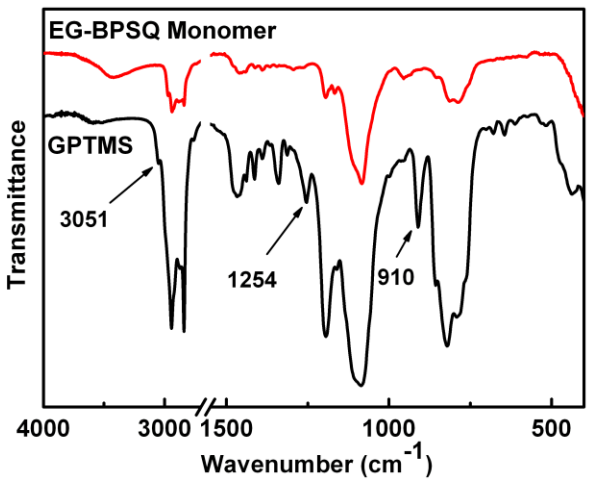

Figure 1. FT-IR spectra of GPTMS and EG-BPSQ monomer.

The stoichiometric reaction between GPTMS and EDA was shown in scheme 1. In the experimental procedure, each nitrogen hydrogen bond of EDA was involved in the ring-opening reaction of the epoxy group of GPTMS. The consumption of GPTMS along its reaction with EDA was characterized by the characteristic peaks of epoxy group in FT-IR spectra. Figure 1 shows the FT-IR spectra of GPTMS and the EG-BPSQ monomer in the range of 400-4000 cm^{-1}. The absorption peak at 3051 cm^{-1} was ascribed to the stretching vibration of epoxy groups $\nu(CH_2)_{epoxy}$ mode, 1254 cm^{-1} was ascribed to the epoxy ring breathing mode, and 910 cm^{-1} was ascribed to the epoxy $\delta_{as}(C_2O)$ mode. The disappearance of these three bands gave strong evidence that the epoxy rings of GPTMS had been opened by the amino groups of EDA and completely consumed in the reaction, because these three bands completely disappeared at the end of the reaction.

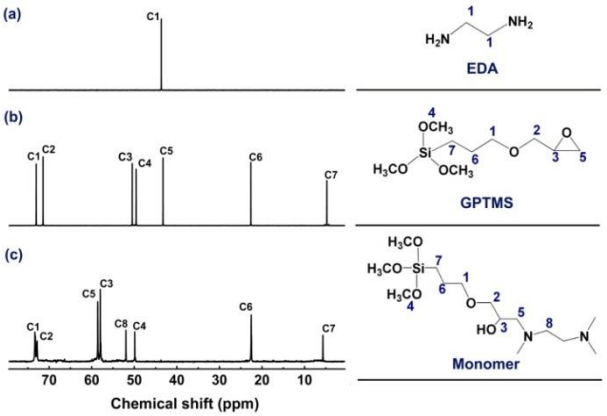

Figure 2. ^{13}C NMR spectra monitoring the EG-BPSQ monomer synthesis process.

^{13}C NMR was employed to disclose the he EG-BPSQ monomer synthesis process. Figure 2 shows the ^{13}C NMR spectra of EDA, GPTMS and the EG-BPSQ monomer. The ^{13}C NMR chemical shifts of EDA, GPTMS and monomer were shown as follows:

EDA, ^{13}C NMR ($CDCl_3$) δ, 44.87 (C1);

GPTMS, ^{13}C NMR ($CDCl_3$) δ, 73.05 (C1), 71.45 (C2), 50.50 (C3), 49.57 (C4), 43.27 (C5), 22.62 (C6), 4.76 (C7);

EG-BPSQ monomer, ^{13}C NMR ($CDCl_3$) δ, 76.36 (C1), 72.84 (C2), 58.00 (C3), 49.90 (C4), 58.60 (C5), 22.53 (C6), 5.70 (C7), 51.83 (C8).

There is only one ^{13}C NMR resonance peak of EDA, which was attributed to the carbon atoms shown in Figure 2a. There are seven ^{13}C NMR resonance peaks of GPTMS, which were assigned to the seven carbon atoms shown in Figure 2b. In Figure 2c, there are eight resonance peaks, corresponding to the eight carbon atoms of EG-BPSQ monomer. The absent peaks at 50.50 ppm (C3) and 43.27 ppm (C5) of GPTMS, and the present peaks at 58.00 ppm (C3) and 58.60 ppm (C5) of the EG-BPSQ monomer clearly indicated that the epoxy ring had been opened by the active hydrogen of EDA, which was in good agreement with the FT-IR results. With the epoxy ring opening, a hydroxyl group was generated on C3 atom and a nitrogen atom was added to C5 atom, which made the chemical shift of C3 and C5 atoms in EG-BPSQ monomer are higher than that in GPTMS. Besides, the present peak at 51.83 ppm (C8) of EG-BPSQ monomer and the absent peak at 44.87 ppm (C1) of EDA indicated that GPTMS had been linked by EDA, and EDA had been completely consumed during the reaction. Based on the above analysis, the chemical structure of the EG-BPSQ monomer could be determined.

Structure of EG-BPSQ gel

RSC Advances Accepted Manuscript

The structure of BPSQ gel was characterized by ^{29}Si MAS NMR. Using this method, different condensation species could be detected. The ^{29}Si MAS NMR signals produced by trifunctional silanes were generally symbolized as T_n, in which n represented the Si-O-Si number linked with a silicon atom, and T_n = Si-(O-Si)$_n$(OR)$_{3-n}$ (n = 0, 1, 2, 3). The degree of condensation (DC) of the BPSQ can be calculated according to the formula: DC (%) = 0.33 * A(T_1) + 0.67 * A(T_2) + A(T_3) , where A(T_n) was the integral area of the T_n specie derived from deconvolution calculation of the ^{29}Si MAS NMR spectrum.

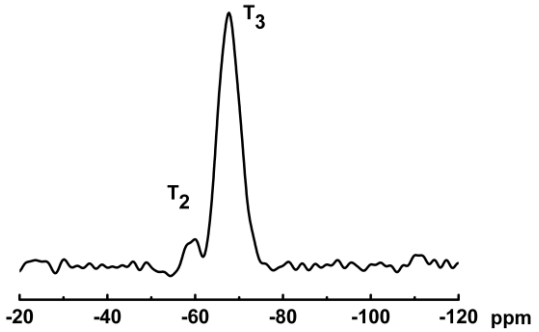

Figure 3. ^{29}Si MAS NMR spectrum of EG-BPSQ gel.

As shown in Figure 3, two peaks are evident in the ^{29}Si MAS NMR spectrum of EG-BPSQ gel. The major peak at -67.7 ppm is the characteristic peak of T_3 specie: Si-(O-Si)$_3$. The minor peak present at -59.9 ppm could be assigned to T_2 specie: Si-(O-Si)$_2$-OH. There was no evidence of T_0 or T_1 species in the ^{29}Si MAS NMR spectrum, indicating that the condensation reaction of silanol groups had proceeded thoroughly. The area under T_3 peak represented 93.8% of the total area, showing a high conversion into Si-O-Si bonds, which illustrated the EG-BPSQ had a high degree (97.9%) of inorganic Si-O-Si polycondensation. As a typical organic-inorganic hybrid material, in EG-BPSQ structure, the inorganic framework was constructed by Si-O-Si structure and the organic networks were composed of flexible carbon chains. The structure of EG-BPSQ gel was showed in Scheme 1. Because many physical and chemical properties of BPSQ are closely related to the molecular structure, length and flexibility of the organic bridge chains. The flexible organic chains of EG-BPSQ cross-linked irregularly in the inorganic framework with high polycondensation degree, which was easier to form the dense structure finally. The surface area of the EG-BPSQ obtained from N_2 adsorption-desorption experiment was 1.17 m^2/g and the pore volume was less than 2×10^{-3} cm^3g^{-1}, illustrating the BPSQ gel was dense and nonporous.

The moisture barrier performance of EG-BPSQ protective film

Two experiments had been designed to test the moisture barrier performance of EG-BPSQ film. The first qualitative method was using allochroic silica gel spheres to test the protective performance of EG-BPSQ coating in underwater environment. The test was carried out as follows: at first, dry allochroic silica gel spheres were coated with EG-BPSQ sol; then, dried for 24 hours at room temperature; finally, the allochroic silica gel spheres were immerged into deionized water till the color changed from blue to pink in water. The result showed that the allochroic silica gel spheres could keep its original blue for more than 24 hours, indicating that the film can prevent the penetration of water effectively. It illustrated that EG-BPSQ film had excellent water-proof performance in water. However, it was not sufficient to conclude that the EG-BPSQ film could also prevent the moisture penetrating effectively. So the next experiment was necessary.

The second experiment was designed to quantitatively check the moisture barrier performance of EG-BPSQ film on KDP crystal in a defined environment, in which the humidity was higher than the real one of KDP crystal application. Figure 4 shows transmittance variation of bare KDP crystals and KDP crystals coated with protective film under relative humidity of 60% at room temperature. Table 1 shows transmittance of bare KDP crystals and KDP crystals coated with protective film at 1053 nm and 351 nm wavelengths in different times under relative humidity of 60% at 25°C. KDP crystal was a water-soluble material and easily affected by damp in atmosphere, resulting in the decline of optical property. Therefore, it was easy to find that the optical transmittance of bare KDP crystal shown in Figure 4a decreased much more seriously than the coated KDP crystal shown in Figure 4b.

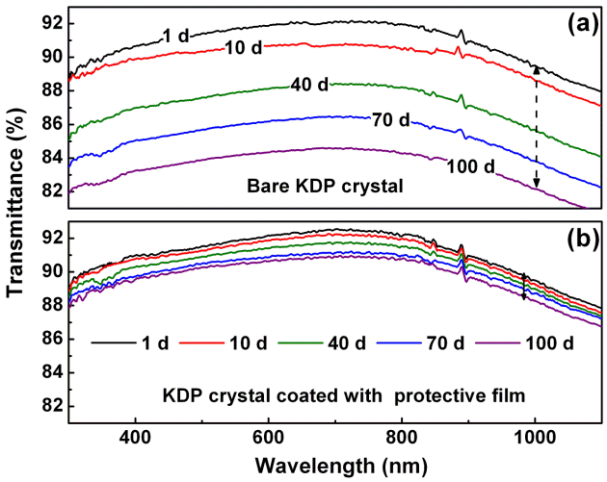

Figure 4. Transmittance variation of bare KDP crystals (a) and KDP crystals coated with protective film (b).

According to Table 1, after 100 days treating under 60% relative humidity, the transmittance of bare KDP crystal decrease from the original 89.90% to 82.60% at 351 nm and 88.54% to 81.32% at 1053 nm, the drop values are 7.40% and 7.22% respectively. Meanwhile, the transmittance of KDP crystal coated with protective film drop only 1.49% at 351 nm and 1.11% at 1053 nm respectively. Based on these results, we can get the conclusion that EG-BPSQ protective film had good moisture barrier performance.

It was worthy to be noticed that the water contact angle of EG-BPSQ film was only 53°, a little higher than that of glass. Thus weak hydrophobicity of EG-BPSQ film was due to the lack of strong hydrophobic groups in the X-bridging organic chain, and the hydroxyl groups introduced by epoxide ring-opening also reduced the hydrophobic property of the EG-BPSQ film. Based on the above results, the good moisture barrier performance of film could be attributed to the dense and

RSC Advances Accepted Manuscript

This journal is © The Royal Society of Chemistry 2012

nonporous structure rather than the hydrophobic property of the film.

Table 1. Transmittance stability of KDP crystal before and after coated with protective film *

Time (days)	Transmittance at different wavelength (%)			
	Bare KDP		Protective film@KDP	
	351 nm	1053 nm	351 nm	1053 nm
1	89.90	88.54	90.40	88.47
10	89.43	87.77	90.19	88.22
40	86.24	84.68	89.49	87.98
70	84.24	82.87	89.24	87.78
100	82.50	81.32	88.91	87.36
Δ T	7.40	7.22	1.49	1.11

*Test condition: relative humidity of 60% at 25℃; Δ T were the transmittance drop values of the different KDP crystals after being treated under relative humidity of 60% at room temperature for 100 days.

The cross-section structure of the protective & AR film

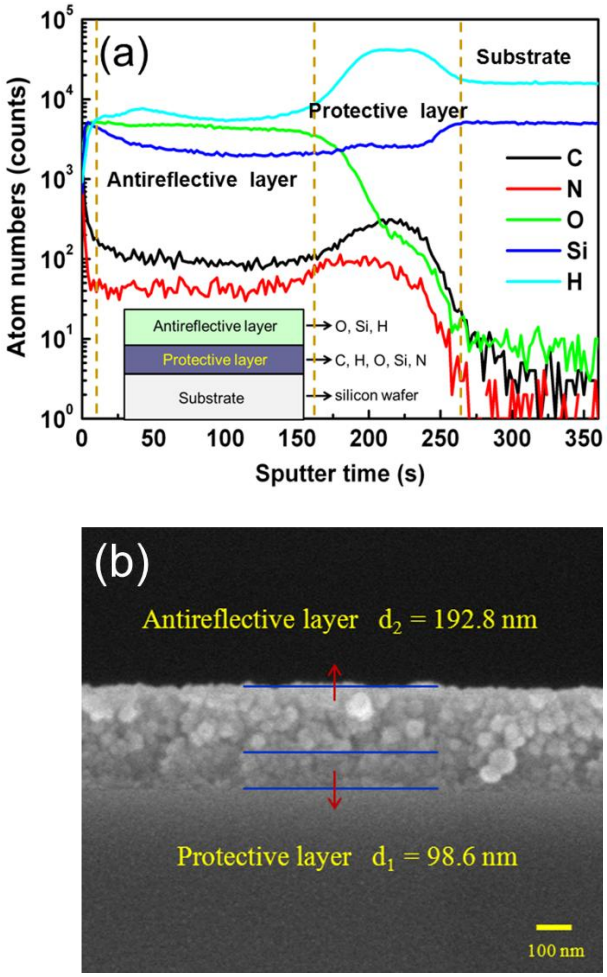

Figure 5. The element distribution through the thickness obtained with ToF-SIMS technique (a) and the cross-section SEM image (b) of the protective & AR double-layer film with central wavelength 1053 nm.

The element distribution through the thickness of the double-layer film was shown by the TOF-SIMS result in Figure 5a. With the extension of sputtering time, the TOF-SIMS signals of all the detected elements show three obviously different evolution stages corresponding to the AR layer, protective layer and Si substrate respectively. At the first stage, the amounts of H, O and Si atoms were significantly higher than that of C and N atoms, which illustrated that the upper layer AR film consisted of H, O and Si elements belonging to SiO_2. The existence of H element revealed that there were many silanol groups (Si-OH) on the surface of SiO_2 particles. With depth extending in the second stage, the amounts of H, C and N atoms obviously increased and the amount of O atoms decreased at the same time. These illustrated that the double-layer film had a clear interface between two different layers.

Figure 5b shows the cross-section SEM image of a double-layer protective & AR film with central wavelength at 1053 nm. To clearly show the interface between substrate and film, the films were coated on a silicon wafer and the cross sections of the film were sprayed by Au nanoparticles prior to SEM imaging. The interface of the two layers could be identified clearly from the image. Moreover, the physical thickness of each layer could be measured easily. The thickness of bottom protective layer was 98.6 nm and the upper AR film was 192.8 nm. Similar TOF-SIMS result can be obtained for the protective & AR double-layer film with central wavelength 351 nm. From the cross-sectional SEM image, its thickness was 67 nm. These result agreed with the thickness measured by the spectroscopic ellipsometer.

The surface morphology of films

Figure 6 shows the AFM images of the single protective film, the single porous silica AR film and the protective & AR film respectively. The root-mean-square roughness, Rq of the bottom layer, upper layer and double-layer film were calculated using the AFM images. To make Rq more precise, the final data was an average roughness of 6 different positions on the surface. From Figure 6a, the surface of the protective film was extremely smooth with Rq less than 1 nm, as low as that of the bare silica substrate. The surface roughness has a direct impact on the surface light scattering. The higher roughness of film is, the stronger surface light scattering will result in the more transmittance decrease of AR film. The very low roughness of the bottom layer implied that the protective film had weak light scattering and no effect on the further preparation of the upper layer. Figure 6b shows the surface of the single upper layer film. Though so many holes and islands are observed, the Rq of the film is 1.36 nm. In fact, the Rq of the double-layer film is only 1.42 nm, which is showed in Figure 6c and almost equal to that of the single upper layer film. This showed that the existence of the bottom layer film had very little influence on roughness of the upper layer film. The bottom layer film was considered as a part of KDP crystal substrate, therefore, the optical transmittance of the double-layer film mainly depended on the upper porous silica AR film.

Optical property of double-layer film

Figure 7 shows the transmittance spectra of the bare KDP crystal, single layer protective film, and the double-layer protective & AR film with central wavelength at 1053 nm or 351 nm. As a frequency converter in high power laser system, KDP crystal was applied to convert the laser wavelength from 1053 nm to 351 nm. That was why the central wavelengths of

RSC Advances Accepted Manuscript

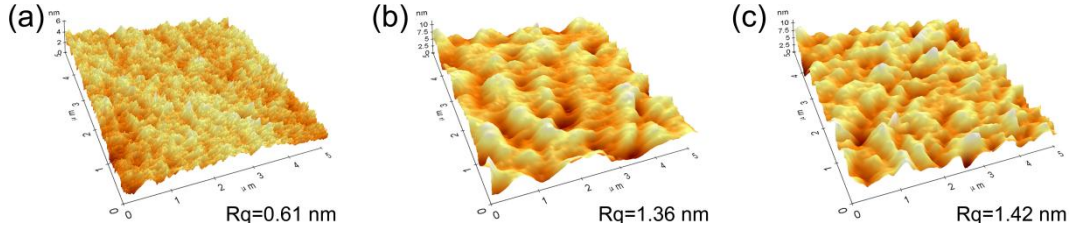

Figure 6. AFM images of films (a) single EG-BPSQ protective film, (b) single AR film (c) protective &AR double-layer film.

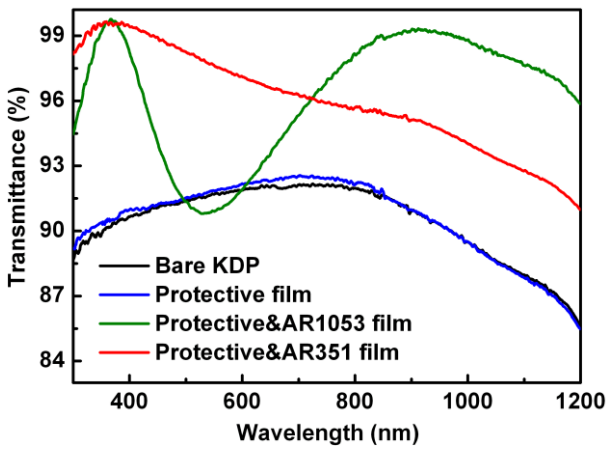

Figure 7. Transmittance spectra of bare KDP crystal and KDP crystal coated with different films.

double-layer antireflective films were selected as 1053 nm and 351 nm rather than others.

The black line shows the transmittance of bare KDP crystal, and the transmittance at 800-1200 nm band was obviously lower than other bands, which was attributed to the intrinsic characteristic of KDP crystal for its function of frequency conversion. EG-BPSQ protective film was a stable, dense and nonporous film, and using it as the bottom layer film could hardly affect the optical performance of the upper layer film. Because the refractive index of the EG-BPSQ protective film was around 1.50, which was close to that of KDP crystal in UV-visible range, the optical transmittance of the protective film was also near to that of bare KDP crystal. Thus the bottom layer film could be considered as a part of the KDP crystal substrate, and, the optical performance of the double-layer film mainly depended on the upper porous silica AR film. Fixing the refractive index of the upper porous silica AR film to 1.19, the AR film with different central wavelength could be obtained only by changing the film thickness. Figure 7 shows that the transmittance of protective&AR351 film reached 99.51% at 351 nm, as shown by red line, meanwhile, the transmittance of protective&AR1053 film reached only 98.09% at 1053 nm, as shown by green line. It was reasonable for the front one because the KDP crystal had no frequency conversion at 351 nm. However, for the latter one, the two transmittance peaks appeared at 361 nm and 912 nm wavelengths, which did not obey the relationship between the fundamental frequency (corresponding to the designed wavelength 1053 nm) and its triple frequency (should be at 351 nm). We attributed the abnormally low transmittance at 1053 nm to the intrinsic characteristic of KDP crystal for its frequency conversion function at this band, which decreased the original peak value at central wavelength of 1053 nm.

The anti-ultraviolet radiation performance of films.

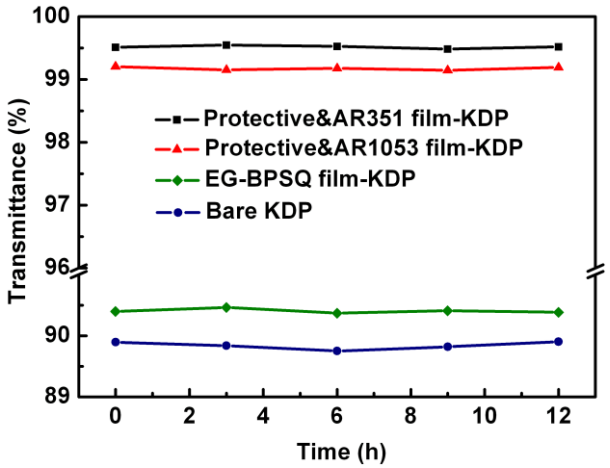

Figure 8. Transmittance variation at wavelength 351 nm of bare KDP and KDP coated with films being irradiated by ultraviolet.

Figure 8 shows transmittance vibration of bare KDP and KDP coated with films at the wavelength of 351 nm after irradiated by an ultraviolet lamp of 300 W. KDP crystal is an inorganic salt whose structure and component would not change after irradiated by ultraviolet light, therefore, the transmittance of bare KDP had no change after being irradiated for 12 h. That was why it was used as frequency converter in high power laser system. KDP coated with either EG-BPSQ film or protective & AR double-layer film had the same result as that of bare KDP. This indicated that the EG-BPSQ film and AR film also had good anti-ultraviolet radiation performance. On the other hand, the result proved that the N-H bonds in EG-BPSQ structure were consumed up in the progress of synthesis EG-BPSQ monomer because ammonia groups were easy to be decomposed by UV light. Based on the above results, the prepared double-layer protective & AR film could satisfy the practical application in UV laser system.

Abrasion-resistance performance of films

Figure 9 shows the transmittance of the KDP crystal coated with EG-BPSQ film before and after being rubbed for 30 cycles by linear abraser with rate of 15 cycles per minute. No obvious reduction in the transmittance of EG-BPSQ film

RSC Advances Accepted Manuscript

 This journal is © The Royal Society of Chemistry 2012

can be observed after being rubbed showing good abrasion-resistance of the EG-BPSQ film. Consequently, the adhesion between EG-BPSQ film and KDP crystal was very strong which was important for practical application. As the upper layer AR film was packed up by SiO_2 nanoparticles, the abrasion-resistance of AR film was somewhat weak. However, the working environment of the double-layer protective & AR film in this paper was in vacuum. Though the adhesion between AR film and EG-BPSQ film was not strong, it could meet the practical application. Nevertheless, we will continue improving the adhesion between EG-BPSQ film and AR film in future work.

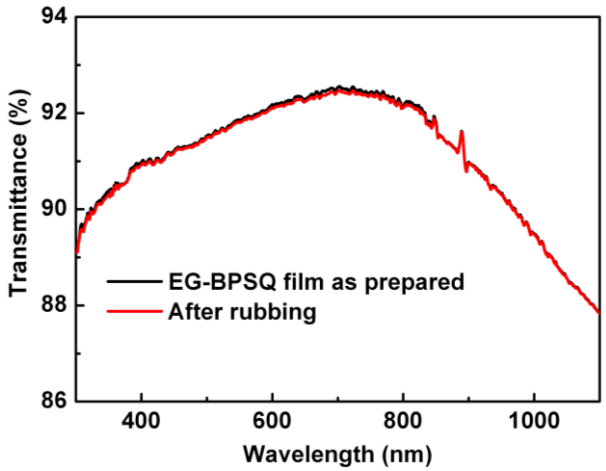

Figure 9. The transmittance spectra of KDP crystal coated with EG-BPSQ film before and after the abrasion-resistance test.

Conclusion

A new X-shape EG-BPSQ monomer was successfully synthesized based on the sol-gel process, according to the stoichiometric reaction between GPTMS and EDA at 60°C without catalyst. Experiment results showed that, the structure of the obtained EG-BPSQ was very dense and had no unsaturated groups, thus, the EG-BPQ protective film possessed good moisture barrier property and anti-ultraviolet radiation performance. In addition, as the bottom layer film, the EG-BPQ film matched well with the upper layer AR silica film. The final double-layer film exhibited excellent moisture barrier and antireflective performance. This method may provide an up gradation to the current KDP protective film, or, an alternation of protective film for other easy deliquescent optical crystals, such as deuterated KH_2PO_4 (KD_2PO_4).

Acknowledgments

Notes

[a] Key Laboratory of Carbon Materials, Institute of Coal Chemistry, Chinese Academy of Sciences, Taiyuan 030001, China.
[b] University of Chinese Academy of Sciences, Beijing 100049, China.
[c] Chengdu Fine Optical Engineering Research Center, Chengdu 610041, China.
*Corresponding author, e-mail: xuyao@sxicc.ac.cn

References

1. H. Tsuji.; T. Tsuruno. *Macromol. Mater.Eng.* 2010, **295,** 709-715.
2. A. R. Millward.; O. M. Yaghi. *J. Am. Chem. Soc.* 2005, **127**, 17998-17999.
3. Yang, L.; Paulson, A. T. *Food Res. Int.* 2000, **33**, 571-578.
4. N. Zaitseva, L. Carman, *Prog. Cryst. Growth Ch.* 2001, **43,** 1-118.
5. I. M. Thomas, *Appl. Opt.* 1992, **28,** 6145.
6. Rigatti, Amy L, Smith, et a1, *Proc. SPIE.* 2001, **4347,** 139-143.
7. X. G. Li, M. Gross, B. Oreb and J. Shen, *J. Phys. Chem. C*, 2012, **116,** 18367-18371.
8. Y. T. Yang, et al. *Materials Letters.* 2008, **62,** 2960-2962.
9. W. D. Wang, et al. ACS nano. 2011, 5, 1267-1275.
10. Q. H. Zhang, *RSC Adv*, 2015, **5,** 4529-4536.
11. H.G. Floch, P.F. Belleville, *Proc. SPIE.* 1992, **1758,** 135-149.
12. K. J. Shea.; D. A. Loy. *Chem. Mater.* 2001, **13,** 3306-3319.
13. Li. Hu.; K. J. Shea. *Chem. Soc. Rev.* 2011, **40,** 688-695.
14. Y. Tokudome, T. Hara, R. Abe and M. Takahashi. *Appl. Mater. Interfaces.* 2014, **6,** 19355-19359
15. A. Chemtob, et al. *New J. Chem.* 2010, **34**, 1068-1072
16. S. W. Hu, Y. Xu, D. Jiang, D. Wu, et al. *Thin Solid Films.* 2009, **518,** 348-354.
17. J. Puig, et al. *Macromolecules*. **2009**, 42, 9344-9350.
18. P. Innocenzi. *J. Sol-Gel Sci Technol.* 2005, **35,** 225-235.
19. P. Cardiano.; P. Piratino, *Polymer.* 2005, **46,** 1857-1864.

RSC Advances Accepted Manuscript